Predicting the Behavior of an Earth and Rockfill Dam under Construction

L. M. Costa[1] and E. E. Alonso[2]

Abstract: This paper presents an application of a coupled hydromechanical formulation for compacted and rockfill materials to simulate the construction and impoundment of a zoned earth dam. The constitutive relation used to model the mechanical behavior of the shoulder, filter and core materials is the Barcelona Basic Model for unsaturated materials. The hydraulic behavior of dam materials requires the specification of their water retention characteristics and their permeabilities, which will be expressed as a function of porosity and degree of saturation. The model was used in the design stage of Lechago's dam (Teruel, Spain), currently under construction. Soil parameters were obtained by laboratory tests performed on materials to be used in the dam. The step-by-step construction (following the sequence construction of nine horizontal layers, besides the downstream preloading layers) and subsequent impounding of the reservoir was simulated in a prediction exercise, which will be hopefully confronted with actual construction measurements in the near future. A parametric study was also performed to evaluate the effects of the compaction water content of the core material on the behavior of the dam.

DOI: 10.1061/(ASCE)GT.1943-5606.0000058

CE Database subject headings: Dams, rockfill; Dam construction; Soil compaction; Unsaturated soils; Finite element method; Predictions.

Introduction

A general review on the evolution of dam's analysis was presented by Fry et al. (1996). First attempts to model consolidation during construction were based on a finite difference technique and included only fluid flow (Richards and Chang 1969). Biot's theory was also applied (Smith and Hobbs 1976). The early consolidation analysis by finite elements of dams considered saturated conditions (Cavounidis 1975) or used uncoupled approaches (Eisenstein and Law 1977), modeling the influence of partial saturation by Skempton's parameters (Skempton 1954).

Ghaboussi and Kim (1982) and Chang and Duncan (1977) presented a formulation valid for unsaturated soils, introducing the interstitial fluid compressibility and maintaining Terzaghi's effective stress principle. Aubry et al. (1987) used a simplified Bishop's effective stress equation. Other authors have also presented coupled analysis considering the soil as a two-phase granular material (Kohgo and Yamashita 1988; Kohgo 1992; Ng and Small 1995).

Naylor et al. (1986) reported a nonlinear elastic analysis of the Beliche dam before it was built. Model parameters were derived from tests on compacted samples, presumably equilibrated at the relative humidity of the laboratory. During construction, Beliche experienced an unexpected wetting due to heavy rains and partial reservoir impoundment and strong settlements developed as a result of the collapse of the dam shells. This effect was not included in the calculations, however. Probably the first attempt to simulate collapse effects in dams by means of a finite element analysis is due to Nobari and Duncan (1972). Their procedure was followed by Veiga Pinto (1983), Justo and Saura (1983), and Soriano et al. (1990). Naylor et al. (1989) generalized the procedure by defining two sets of constitutive parameters, for dry and saturated conditions. They later applied it to an *a posteriori* analysis of the Beliche dam (Naylor et al. 1997). They used an elastoplastic critical state model and a total of 14 constitutive parameters had to be used. The procedure, however, is unable to follow dam deformations during the history of dam wetting.

One of the first applications of unsaturated soil models to dam analysis considering a three-phase soil was reported by Alonso et al. (1988). Soil deformations were simulated by state surface concepts (Matyas and Radhakrishna 1969; Lloret and Alonso 1985). A similar approach was also applied later by Alonso and Batlle (1995) and Alonso et al. (1995) in the simulation of earth dam construction and long-term behavior. Laigle et al. (1995) considered a three-phase soil, and used a stress-strain hyperbolic model and a coupled behavior on the simulation of the La Ganne dam. One of the first applications of an elastoplastic model to analyze the construction of an homogeneous earth dam was presented by Bonelli and Poulain (1995). The development of pore pressure was examined in terms of placement water content. Their formulation was limited to undrained events.

Fully coupled analysis of earth and rockfill dams using two independent stress fields (suction being one of them) have been performed by Costa (2000), Kogho (2003), and Alonso et al. (2006).

This paper presents an application of coupled hydromechanical models, developed for unsaturated soil, to the analysis of a

[1]Professor, Civil Engineering Department, Federal University of Pernambuco, Av. Acadêmico Hélio Ramos, s/n, 50740-530, Recife-PE, Brazil.

[2]Professor, Department of Geotechnical Engineering and Geoscience, Technical University of Catalonia, Campus Nord, Building D2, Jordi Girona 1-3, 08034, Barcelona, Spain.

Note. This manuscript was submitted on September 15, 2007; approved on October 20, 2008; published online on February 21, 2009. Discussion period open until December 1, 2009; separate discussions must be submitted for individual papers. This paper is part of the ***Journal of Geotechnical and Geoenvironmental Engineering***, Vol. 135, No. 7, July 1, 2009. ©ASCE, ISSN 1090-0241/2009/7-851–862/$25.00.

zoned earth dam currently under construction (Lechago's dam in Teruel, Spain). Lechago's dam design presents some unique features; a preloading stage was designed to improve the strength of the soft foundation soils and, in addition, a soil treatment to increase foundation stiffness by means of treated soil columns was also envisaged in order to homogenize foundation conditions of the clay core throughout the cross section of the valley. Both aspects were modeled.

The dam compacted core, filters, and shoulders have been modeled by means of an elastoplastic model for unsaturated materials. Material parameters have been derived from laboratory test results. The predicted dam behavior cannot be compared at present with field measurements, but the analysis presented here may be considered as a blind prediction exercise, which will eventually be compared with actual observations. In addition to this objective, the paper highlights the benefits of a modern coupled analysis using elastoplastic constitutive models for unsaturated soil conditions if compared with other approaches mentioned above. This point is discussed with reference to an important aspect of dam design: the selection of compaction conditions. It will be shown that compaction conditions are included in the analysis through the initial conditions defined in terms of the stress variables selected to define the constitutive model. The classical compaction variables (dry unit weight and water content) are expressed in terms of stresses. The definite advantages of this approach are discussed and are exemplified through a sensitivity analysis on the effect of compaction conditions on the response of Lechago dam clay core.

Hydromechanical Behavior of Unsaturated Soils

In a general isothermal formulation two equations of mass conservation (for water and air species) and a set of equations for stress equilibrium should be solved. This approach has been followed by Gatmiri et al. (1995) and Ledesma et al. (1995). A recent modern formulation may be found in Olivella et al. (1994, 1996). A general purpose finite element simulator (CODE_BRIGHT), developed in recent years, solves this system of equations under fairly general conditions. A detailed account of CODE_BRIGHT, its theoretical background, and numerical structure is given in DIT_UPC (2002).

Hydraulic Constitutive Equations

Water and air flow are modeled by generalized Darcy's laws

$$v_w = \boldsymbol{K}_w(\nabla p_w - \rho_w g) \tag{1}$$

$$v_a = \boldsymbol{K}_a(\nabla p_a - \rho_a g) \tag{2}$$

where $\boldsymbol{K}_w$, $\boldsymbol{K}_a$=permeability tensors; p_w and p_a=water and air pressure, respectively; ρ_w and ρ_a=water and air density, respectively; and g=acceleration due to gravity.

Air and water permeability are nonlinear functions of porosity n and degree of saturation S_l. In this paper, permeability is related to degree of saturation and soil porosity by means of

$$\boldsymbol{K} = \frac{\mathbf{k} k_{rl}}{\mu_l} \tag{3}$$

where

$$\mathbf{k} = \mathbf{k}_{\text{ref}} \frac{n^3}{(1-n)^2} \frac{(1-n_{\text{ref}})^2}{n_{\text{ref}}^3} \tag{4}$$

$$k_{rl} = S_e^{\alpha} \tag{5}$$

where $\mathbf{k}$=intrinsic permeability tensor; $\mathbf{k}_{\text{ref}}$=intrinsic permeability for a reference porosity n_{ref}; μ_l=liquid viscosity; and k_{rl}=relative permeability. The effective degree of saturation S_e =function of the current degree of saturation S_l, given below, and α=constant (close to 3).

The relationship between suction and degree of saturation is described by the retention curve, which in this work is modeled by the Van Genuchten (1980) expression

$$S_e = \frac{S_l - S_{rl}}{S_{ls} - S_{rl}} = \left[1 + \left(\frac{p_a - p_w}{P_0}\right)^{1/(1-\lambda)}\right]^{-\lambda} \tag{6}$$

where P_0 and λ=material parameters for the retention curve; S_{rl} =residual saturation; S_{ls}=maximum degree of saturation; and s $=p_a-p_w$ is the matric suction.

Mechanical Constitutive Equations

Advances in the understanding of unsaturated soil behavior have shown that the complex behavior of these materials is better understood and described within the framework of hardening plasticity (Alonso et al. 1987; Alonso et al. 1990). Among the several elastoplastic models developed during the last decade, the Barcelona Basic Model (BBM; Alonso et al. 1990) remains as a reference model which combines simplicity and a good capability to reproduce fundamental aspects of unsaturated soil behavior. It is the model adopted in this paper.

BBM explains the following set of experimental observations in compacted materials: yield stresses increase with suction; after wetting-induced collapse the soil state ends in the saturated compression line; wetting paths lead to a variety of responses [pure (elastic) swelling, initial swelling followed by compression and monotonic collapse]; strength increases with suction and it follows critical state conditions for constant suction. It has a number of limitations: it is not coupled with hydraulic effects (suction has to be independently related with water content and stress state); it is not appropriate to describe expansive soils (in particular, swelling strains are not prevented by confining stresses within the elastic region); it does not consider anisotropy [inherent or induced) by the applied stress path; and it includes also the limitations of modified Cam-clay (hardening is isotropic and volumetric, no kinematic hardening, and an inaccurate representation of yield locus for high over consolidation ratio (OCRs)]. It does not consider either some advanced features found in some constitutive models for saturated soils (small strain behavior, ability to model cyclic application of stress and creep effects).

Under isotropic conditions, the model uses two independent stress variables: the net stress ($\sigma_{ij}-p_a\delta_{ij}$) and matric suction s. A synthetic description of BBM is given in the Appendix.

Design of Lechago Earth Dam

The Lechago dam is being built in Aragón, northeastern Spain, for irrigation purposes. The design presented some difficulties due to the existence of a highly compressible and low strength layer in the river alluvium and the nonsymmetric cross section of the valley. This led to specify the utilization of a preloading downstream

J. Geotech. Geoenviron. Eng., 2009, 135(7): 851-862

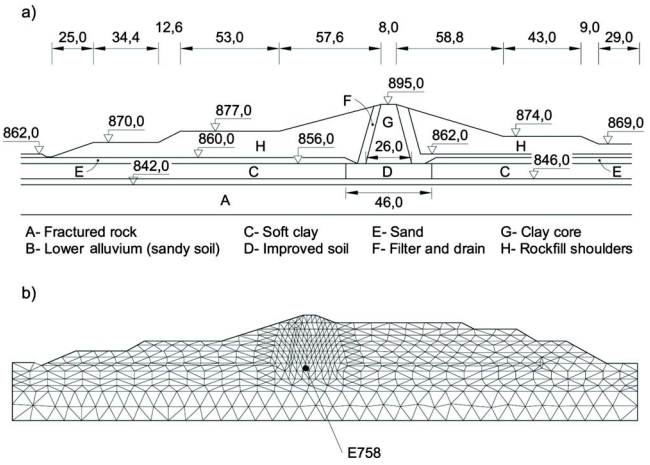

Fig. 1. (a) Cross section of Lechago dam; (b) finite-element mesh

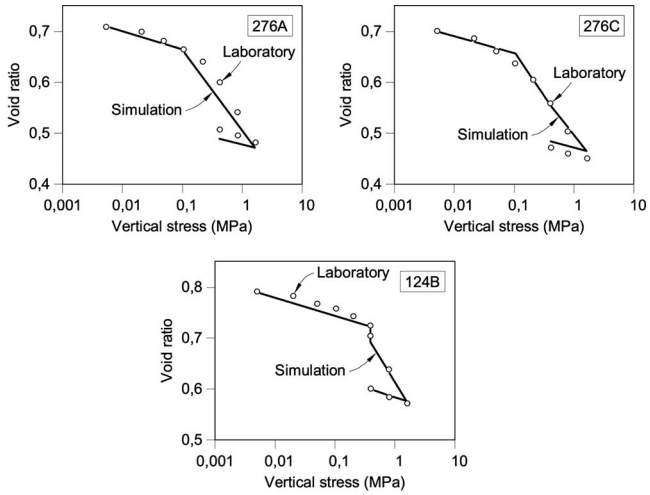

Fig. 2. Measured compression curves and model predictions for three compacted specimens of clay intended for the dam core

of the dam axis in order to improve the strength of the foundation clay layer. The design also establishes an improvement of the soft clay layer by means of soil treated columns with the purpose of limiting the dam core settlement. The sharp transitions between the soft alluvial deposits and the shaly abutements may otherwise lead to unacceptable differential distortions.

The alluvial foundation deposit can be divided in three layers: an upper sandy layer having medium relative density, an intermediate low plasticity soft clay layer of deltaic origin, classified as CL, and a lower granular layer on top of the underlying fractured shale.

As defined in the design, the dam will have a central compacted clay core, protected by granular filters and wide rockfill shoulders. A representative cross section of the Lechago dam is given in Fig. 1(a).

Constitutive Models for Dam and Foundation Materials

Dam Materials

The material selected for the core is a low plasticity red silty clay of tertiary origin (w_l=35%; w_p=17.6%), which presents a dry density of 18 kN/m^3 and optimum water content of 14.5% when compacted under Normal Proctor compaction conditions. A series of conventional oedometer and wetting inundation tests were carried out with compacted samples in order to determine the clay core properties.

Samples from different potential quarry locations, all of them within the same geological unit, were collected. Specimens were compacted under Normal Proctor conditions. Four groups of samples were tested under oedometric conditions. A total number of 11 tests were performed. Different wetting histories were imposed on the samples. In some tests the effect of water saturation was simulated by soaking the specimen at constant vertical stress. All of the measured void ratio–net vertical stress relationships were simulated by means of BBM. Fig. 2 shows a comparison between model predictions and actual compression curves for three specimens. Samples 276A and 276B were soaked at 100 kPa, while sample 124B was soaked at 400 kPa. Specimens from one location exhibited a significantly higher stiffness [as reflected in the $\lambda(0)$ virgin compression coefficient] than the others. This result could be related to the higher sand content of specimens from that particular location. The remaining tests could be reasonably reproduced with $\lambda(0)$ values in the vicinity of 0.068, as Fig. 2 indicates.

Compression coefficients for virgin loading and unloading-reloading [$\lambda(0)$ and κ] could be directly derived from compression curves. Other parameters of BBM, namely, p^c, p_0^*, r, β, and κ_s required a back-analysis identification procedure through the model itself.

Original BBM was formulated for a constant compressibility elastic parameter. However, there is extensive experimental evidence on the effect of suction on elastic soil parameters (Gens et al. 1997; Alonso 1998). Accordingly, κ was made dependent on suction through the equation

$$\kappa_i = \kappa_0(1 + \alpha_i s) \tag{7}$$

where κ_0=reference value, for null suction; and α_i=constant.

Triaxial tests on saturated compacted samples were used to determine the critical state slope M. Elastic shear stiffness G was derived from the current value of κ_i, assuming a constant Poisson's ratio ν. It depends on mean stress p and void ratio e through

$$G = \frac{3(1-2\nu)}{2(1+\nu)}\frac{p(1+e)}{\kappa} \tag{8}$$

The identified material parameters for the core material on the basis of the tests performed are summarized in Table 1. A small increase in apparent cohesion with suction (k=0.1) was also assumed.

One of the major challenges of rockfill modeling, in connection with dam behavior, is the consistent representation of volumetric deformations due to water content changes. Some features of rockfill behavior, i.e., increased stiffness of the dried material and the collapse upon wetting, are also observed in low activity unsaturated soils with a relatively open structure. However, underlying mechanisms are widely different in both cases since capillary effects are irrelevant in large-size particles.

Recent research on the basic mechanisms of rockfill compressibility (Oldecop and Alonso 2001) has shown that rockfill behavior could be interpreted in terms of the rock basic properties and fracture propagation phenomena. Beyond a certain threshold confining stress, rockfill irreversible deformations are explained by particle breakage. For a given rockfill arrangement, particle

J. Geotech. Geoenviron. Eng., 2009, 135(7): 851-862

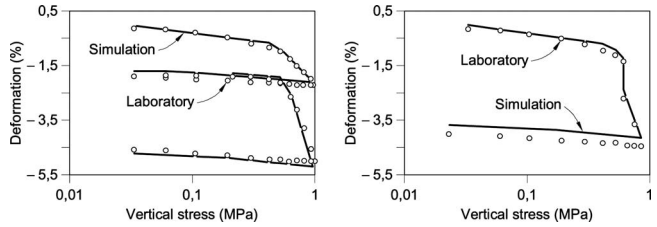

Fig. 3. Measured compression curves and model predictions for two compacted specimens of scaled rockfill intended for dam shoulders

breakage is controlled by the prevailing relative humidity in the open pores of rockfill. In fact, water acts as a corrosion agent, and its chemical potential (or water suction) determines the velocity of particle breakage. Particle breakage leads to rearrangements of the rockfill structure and eventually to macroscopic irreversible strains.

Oldecop and Alonso (2001) showed that these basic ideas could be cast in terms of an elastoplastic framework in order to model rockfill compressibility. The model developed has formal similarities with BBM, even though the underlying deformation mechanisms are widely different. In fact, the basic BBM has useful potential to describe rockfill compressibility. If used in this context, suction loses its interpretation as a capillary induced internal isotropic stress and becomes simply a description of the state of energy of the water in rock particle pores.

Several large scale oedometer tests (30 cm diameter) were performed in a Rowe type cell with humidity control. The soil tested was a scaled rockfill granular material. Particle sizes varied between 1 and 5 cm. Crushed rock samples were taken from outcrops of quartzitic shale at the location of the Lechago dam. This material, widely available at the site, will be used in shoulder construction. Samples were compacted in the cell in several layers with a compaction energy equivalent to the energy of a Proctor Normal test.

The five oedometer tests performed involved loading-wetting-unloading sequences which have been described in detail elsewhere (Oldecop and Alonso 2001). The results of two of such tests (Tests 2 and 4) are shown in Fig. 3.

It turned out that BBM was capable of modeling quite precisely the tests performed. Parameter identification for the isotropic part of BBM followed techniques outlined for the interpretation of tests on compacted clay samples. No triaxial tests were, however, performed on this crushed rock material and a value $M=1.6$ was assumed. Large diameter triaxial tests on compacted gravel of Lechago shale, reported in Chávez and Alonso (2003), indicated that M varies between 1.5 and 1.7 when relative humidity (RH) conditions change between RH=100% and RH=36%. Cohesion was assumed to be essentially zero. Since a small elastic expansion of the rockfill material was observed, when relative humidity increased, a small (constant) value of κ_s was specified. The set of material constants for the rockfill are also shown in Table 1.

Table 1. Constitutive Parameters for Dam Materials

	Core	Filter	Shoulder
Elastic			
κ_0	0.019	0.004	0.004
κ_s	0.004	0.005	0.005
ν	0.3	0.3	0.3
α_{is}	−0.05	0.0	0.0
Plastic			
$\lambda(0)$	0.068	0.072	0.082
r	0.75	0.20	0.20
β (MPa^{-1})	3.0	35.0	35.0
k	0.1	0.01	0.01
M	1.0	1.4	1.6
p_0^* (MPa)	0.08	0.42	0.42
p_c (MPa)	0.01	0.41	0.41
α	0.493	0.454	0.440

Table 2. Hydraulic Properties of Dam Materials

	Core	Filter	Shoulder
Intrinsic permeability			
k_0 (m^2)	3.0×10^{-17}	4.0×10^{-13}	2.0×10^{-13}
n_{ref}	0.377	—	0.365
Retention curve			
P_0 (MPa)	1.0	0.01	0.01
λ	0.18	0.6	0.6

Filter materials play a limited role on the overall mechanical behavior of the dam. No tests on these materials were available and its properties were directly based on the set of constitutive parameters determined for the scaled rockfill. The changes introduced reflected the following design specifications: filter stiffness should be lower than rockfill stiffness (but higher than core stiffness) and its average friction angle should be close to $\varphi'=35°$. Table 1 indicates the set of adopted physical parameters for the filter layers. Hydraulic conductivities and water retention characteristics were approximated with the material constants shown in Table 2.

Foundation Materials

Natural foundation soils at the cross section of maximum dam elevation consisted, from top to bottom, of an upper 5 m thick layer of sandy soil, followed by a 10 m thick soft clay deposit, a lower 5 m thick sandy layer, and a fractured shale bedrock. Linear elastic models were adopted for the sandy layers and the lower rock substratum. The sand levels were found to be rather compact. An average elastic modulus $E=500$ MPa was assigned to them. Their importance in the behavior of the dam is minor and it was not deemed necessary to adopt a more involved nonlinear model for them. However, the soft clay was modeled by a modified Cam-clay model. A water table was located at 5 m deep from the surface.

Oedometer and triaxial tests were performed on samples recovered from the clay deposit. The soft clay has a low plasticity ($w_l=25\%-35\%$) and void ratios in the vicinity of $e_0=0.7$. Cone penetration test with pore-pressure measurement (CPTU) tests (including dissipation tests at some points within the clay layer) were also available. From oedometer consolidation tests, the following compression coefficients were derived: $C_c=0.17$; $C_s=0.03$. From them, $\lambda(0)=0.07$ and $\kappa_0=0.014$. A critical state friction angle $\varphi'=20°$ ($M=0.8$) was also determined. The value of C_c is consistent with correlations reported by Holtz and Kovacs (1981) in terms of e_0 and clay plasticity.

The profile of mean preconsolidation stress was approximated by two constant values: $p_0^*=0.18$ MPa in the upper 5 m and p_0^*

J. Geotech. Geoenviron. Eng., 2009, 135(7): 851-862

Table 3. Cam-Clay Parameters for Foundation Clay Layer and Improved Foundation Soil

	Clay layer	Improved soil
Elastic		
κ_0	0.014	0.014
ν	0.3	0.3
Plastic		
$\lambda(0)$	0.07	0.05
M	0.8	0.8
$p^*_{0(1)}$ (MPa)	0.18	0.18
$p^*_{0(2)}$ (MPa)	0.28	0.28

=0.28 MPa in the lower 5 m sublayer. Saturated permeability was derived from the average coefficient of consolidation obtained in CPTU dissipation tests (c_v=6 cm^2/min). The estimated intrinsic permeability was 1.5×10^{-15} m^2.

As mentioned before, the project specifies a zone of treated clay soil below the dam core in order to reduce the distortion of the dam in rock-alluvium transitions. Lime columns were designed to achieve the intended improvement in clay stiffness. However, designers were concerned by the possibility of the lime columns to damage the clay core during dam settlement. The design specified that the lime columns would not rest on the rigid substratum but, rather, they would remain as floating piles. Their effect was estimated by an average compression index $\lambda(0)$ =0.05. The improved soil, considered as a homogenized material was also described by means of a modified Cam-clay model. The remaining soil parameters were not modified, as Table 3 indicates. Permeability of the improved soil was increased by an order of magnitude as some experience with treated soils indicate (intrinsic permeability was estimated as 1.5×10^{-14}m^2).

For the two granular layers and the lower fractured rock, an isotropic linear elastic model is defined by its elasticity modulus E and Poisson's ratio ν. Intrinsic values of permeability were determined from *in situ* pumping tests. The values adopted are listed in Table 4.

Dam Analysis

General Features

A specific feature of the Lechago's dam project is a preloading phase of the downstream foundation in order to meet the safety requirements against short term downstream sliding failure at full reservoir level. Preloading was integrated into dam construction; rockfill is to be accumulated on the downstream shoulder up to an elevation close to the elevation of the core axis. In the simulation performed, dam and preload construction is modeled by means of horizontal layers whose sequence of installation is: the first seven loading steps correspond to the dam itself, whereas steps 8 to 15 belong to the downstream preloading. The dam is finished when step number 16 is finally added. The removal of preloading layers begins 6 months after dam and preloading construction ends.

Table 4. Elastic Parameters for Granular Foundation Layer and Fractured Rock

Material	E (MPa)	ν	K (m^2)	n_0
Granular layer	500.0	0.3	1.2×10^{-13}	0.3
Fractured rock	5000.0	0.3	1.0×10^{-14}	0.1

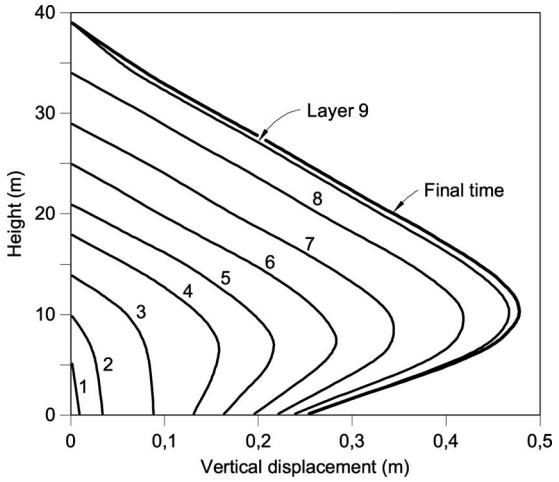

Fig. 4. Vertical settlements along the dam axis during construction

Fig. 1(b) shows the finite-element mesh in its largest size (1077 triangular elements and 487 nodes). A total of nine horizontal layers whose thickness varies between 3 and 6 m were defined. Construction or excavation is simulated by "switching" on or off a set of elements. Excavated elements are assigned negligible values of stiffness, gravity, and permeability. When an element is being built or activated, its properties are switched on to the values shown in Tables 1 and 2.

The lower boundary of the discretization is assumed to be fixed and impervious. Upstream and downstream ends of the foundation layers are also restrained to move in a horizontal direction and are considered impervious. Initial conditions for foundation elements are simple: a geostatic total stress distribution and a hydrostatic water pressure. Built elements are assigned a small arbitrary initial stress to avoid instabilities in the nonlinear constitutive equations. Concerning suction, an initial value of 3 MPa was assigned to elements of the clay core. For filter and rockfill elements, initial suction was taken as 0.05 MPa. Given the low value of the air entry value for these coarse granular materials (P_0=0.01 MPa; Table 2), this initial suction results in a very low saturation.

Dam Construction

The dam (and the downstream preload) was built in 6 months. At this time, primary consolidation of the soft foundation clay layer is essentially complete. The preload was removed in 14 months (2 months for each layer). The results presented here correspond to this particular time.

Pore water pressures in the core reflect two phenomena: the progressive increase in stress due to dam construction and the interaction with the filters. The suction gradient at the core-filter interface explains the moderate nonhomogeneity of water pressure in the core. The core maintains negative pore water pressures except at lower elevations where positive pressures are computed. The degree of saturation of the core remains in the range from 0.8 (at top level) to 1 at the lower elevations.

Typical distribution of vertical settlements of the core axis for different construction stages are plotted in Fig. 4. The position of maximum settlement (which evolves from locations at the core-

J. Geotech. Geoenviron. Eng., 2009, 135(7): 851-862

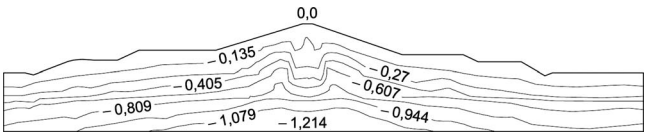

Fig. 5. Vertical stress contours at the end of construction (MPa)

foundation contact to points in the lower third of the dam height) reflects foundation deformations as well as the varying core stiffness induced by suction distribution.

Contour plot of vertical stresses (Fig. 5) provide a good indication of dam behavior during construction. The core-shoulder transition in stiffness results in stress redistributions (arching) as shown in Fig. 5. Stress distribution away from this interface is essentially controlled by vertical equilibrium as the same figure points out.

The set of results presented before may be described as conventional since similar trends are derived from standard elastoplastic analysis. However, a deeper insight may be gained by exploring the stress paths followed by some soil elements during construction. Fig. 6 shows the (p,q) and (p,s) stress paths calculated for an element centered in the first layer of the clay core [first step in Fig. 1(b)]. The initial stress state corresponds to a compacted state characterised by a suction of 1 MPa and a negligible stress intensity. As new layers accumulate on top, suction decreases and, at the same time, mean and shear stresses build up. The stress path remains initially in the elastic region [initial ellipse and loading-collapse (LC) yield loci are also shown in Fig. 6]. Note also that the initial suction induces a significant apparent cohesion of the soil. Eventually, the stress path hits the yield surface when suction is close to 0.4 MPa. Beyond this point volumetric deformations have four components: a (small) swelling strain due to further suction reduction, a collapse of the soil structure due to the displacement of the LC yield curve, an elastic compression due to increment of confining stress and a dilatancy component due to plastic yielding.

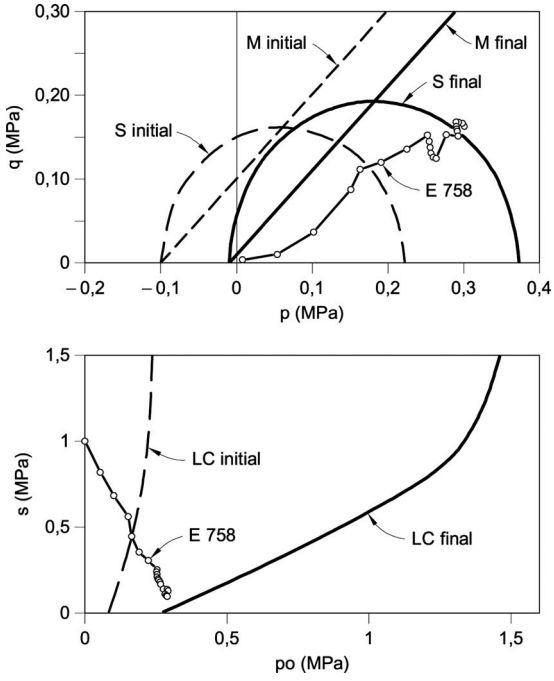

Fig. 6. Stress path of element 758 (core) in (p,q) and (p,s) planes

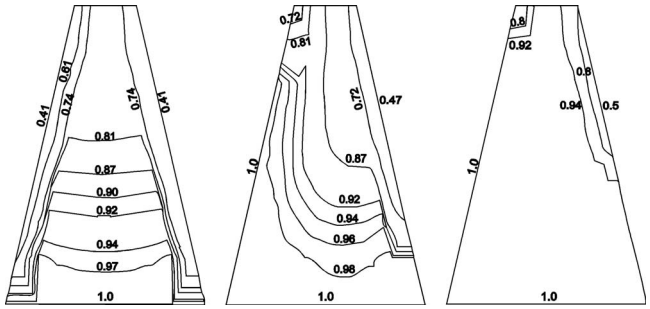

Fig. 7. Evolution of degree of saturation in the core at the beginning of impoundment (left), at an intermediate time (center), and at steady-state conditions (right)

The stress path plotted reflects also the removal of preloading downstream and the transient flow regime during the whole process. The final stress point is in a yield condition very close to saturation but away from the critical state. Note also how the apparent soil cohesion decreases as suction increases. During the construction and preloading sequences the saturated preconsolidation mean stress evolves from the initial value $p_0^*=0.08$ MPa to a final value of $p_0^*=0.27$ MPa. This increase is associated with a plastic volumetric strain of 3.5%.

Reservoir Impounding

Impounding is simulated by applying a surface total stress of (γ_w,h_w) in the direction perpendicular surface and also setting the boundary pore water pressure to be (γ_w,h_w) at the upstream shoulder contour nodes in contact with water. Surface total stress and water pressure are imposed in a specific node at the moment that water level reaches the node coordinate. From this moment on they are updated with the expected water level evolution.

Boundary conditions are the same as those used in construction, except for a new variable condition, which is introduced in the upstream contour where surface total stress and water pressure are prescribed. The initial stress state is now given by the final construction stage.

Infiltration through the core due to impoundment is illustrated in Fig. 7. The wetting front developed can be seen by the degree of saturation contours at three different times after impounding. The wetting front (identified as the contour of $S_l=1$) enters the core as a surface approximately parallel to the upstream interface between rockfill and core. Later it adopts the classical saturation line typical for steady-state conditions

Hydraulic fracture risk was analyzed by comparing the values of total minor principal stress (σ_3) and water pressure (p_w) at points in the upstream interface of the core. Table 5 presents the results for some boundary elements at different times during impounding. A safety factor is defined as the ratio σ_3/p_w. It is observed that the intermediate time t_2 corresponds to the worst situation in terms of hydraulic fracture risk. An increase of water pressure corresponds to an increase in minor principal stress. The results indicated that the increase in minor principal stress can be higher than the development of water pressure. Fig. 8 shows the evolution of the safety factor against hydraulic fracture with time.

Infiltration leads to a fast reduction of suction of the upstream shoulder and to the reduction of effective stresses. The process of

J. Geotech. Geoenviron. Eng., 2009, 135(7): 851-862

Table 5. Comparison between Water Pressure and Minor Principal Stress and Calculated Safety Factors

	Intermediate time t_1			Intermediate time t_2			Steady-state condition		
Element	p_w (MPa)	σ_3 (MPa)	FS (σ_3/p_w)	p_w (MPa)	σ_3 (MPa)	FS (σ_3/p_w)	p_w (MPa)	σ_3 (MPa)	FS (σ_3/p_w)
733	0.213	0.282	1.324	0.229	0.308	1.345	0.243	0.357	1.469
726	0.154	0.178	1.156	0.183	0.202	1.104	0.206	0.264	1.282
706	0.089	0.119	1.337	0.134	0.137	1.022	0.168	0.214	1.274
695	0.02	0.083	4.150	0.074	0.089	1.203	0.132	0.17	1.288

suction reduction in the core is essentially controlled by clay unsaturated/saturated permeability. In both cases the resulting volumetric deformations include several components: A (small) heave due to suction reduction, a plastic collapse and, when the soil becomes saturated, elastic rebound due to the effect of effective stress reduction. This is a somewhat simplified view because shear components may also lead to dilatancy effects at some points and, also, total stress changes also occur. The end result, in terms of calculated settlements is shown in Fig. 9. Calculated settlements of the shell are small. The core reaches a maximum settlement of around 27 cm.

Effect of Compaction Water Content in Core Behavior

Compaction states are defined in practice by the dry specific weight (γ_d) and the water content (w). Properties of compacted soils are expected to change when the pair (γ_d, w) changes. However, it is not simple to provide a systematic quantitative description of the mechanical behavior of different compaction states unless a comprehensive testing program is undertaken.

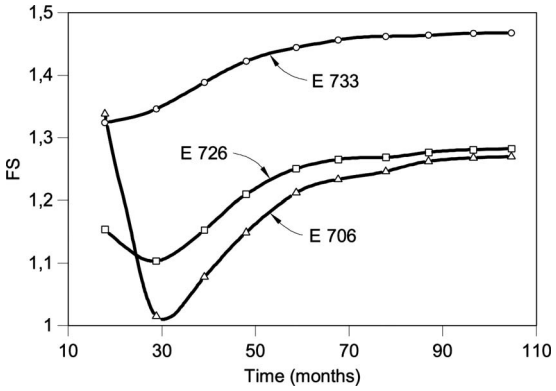

Fig. 8. Evolution of the safety factor against hydraulic fracture with time

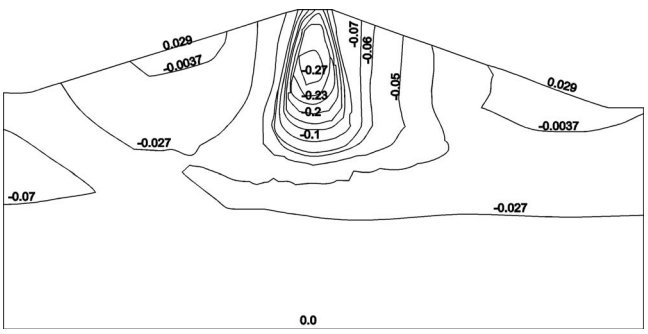

Fig. 9. Settlement contours due to impounding (m)

Unsaturated soil mechanics offer a powerful alternative to estimate the properties of compacted soils. The following discussion is based on the constitutive model BBM, described in the Appendix. The first step is to recognize that the information provided by the compaction variables (γ_d, w) may be advantageously substituted by a pair of stress variables: the (saturated) effective mean yield stress p_0^* and the soil matric suction s. The compaction process is a procedure to induce irreversible deformations in the soil. In this sense, the maximum compaction stress (if induced statically) or compaction energy may be interpreted as an equivalent yield or preconsolidation stress. It is then natural to accept that the attained dry specific weight is univocally related to a yield stress. The higher the dry density, the higher p_0^*. Relationships of this type have been reported in Alonso and Pinyol (2008) for a variety of compacted soils.

The pair (γ_d, w) also defines the degree of saturation. As a first approximation, a given S_l will be related (through the water retention curve) with the soil suction. Therefore, the pair (γ_d, w) could be substituted by the pair (p_0^*, s). This equivalence has fundamental implications because it opens the possibility of introducing in an "automatic" manner the change in properties of compacted soils when compaction conditions change. This, in turn, provides a simple and powerful procedure to examine the effect of changing compaction conditions at design stage. The condition, though, is that compacted soil behavior is modeled through a consistent constitutive model for unsaturated soils, such as BBM. Further discussion on this topic is given in Sivakumar and Wheeler (2000).

In fact, the specification of BBM for a particular soil requires the identification of a number of material parameters (described in the Appendix) and the initial conditions. The initial conditions are precisely given by p_0^* (which marks the position of the yield locus LC) and by the stress state. Since the model is formulated in terms of net stress and suction, the initial value of the pair (p, s) (isotropic conditions) or (p, q, s) (triaxial conditions) should be specified. The state of stress (p, q) is initially a low value (it corresponds to the stress state in a layer just extended). Suction depends on (γ_d, w) and on the water retention properties of the soil.

These comments are illustrated in Fig. 10 for isotropic stress states. Fig. 10(a) indicates six compaction states belonging to two compaction energies. Also indicated are the loci of equal degree of saturation. The ideas discussed above allow representing immediately the initial state of the six compaction conditions in Fig. 10(b). Three different suction values, i.e., high (dry of optimum), medium (optimum), and low (wet of optimum), are plotted. In all cases a small initial net mean stress is accepted. The attained dry density is reflected in the p_0^* value indicated. The model parameters of the constitutive model (BBM) (which in a first approxi-

J. Geotech. Geoenviron. Eng., 2009, 135(7): 851-862

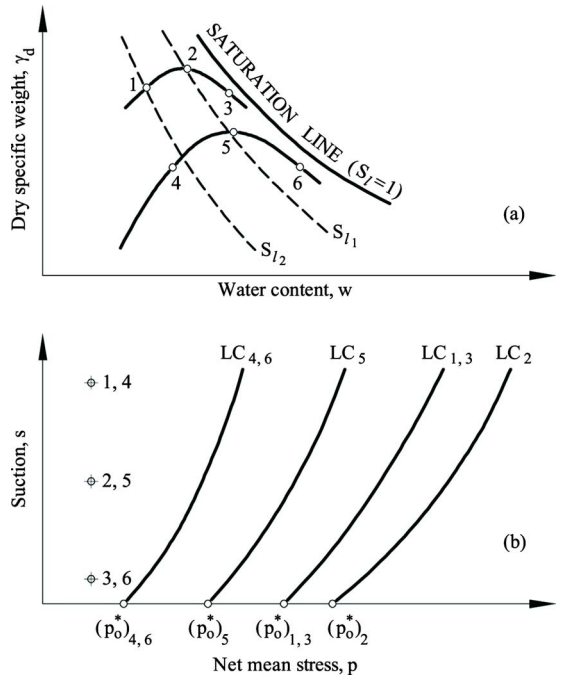

Fig. 10. Compaction conditions and constitutive model BBM (isotropic conditions): (a) different compaction conditions in (γ_d, w) plane; (b) equivalent conditions in (p, s) stress space

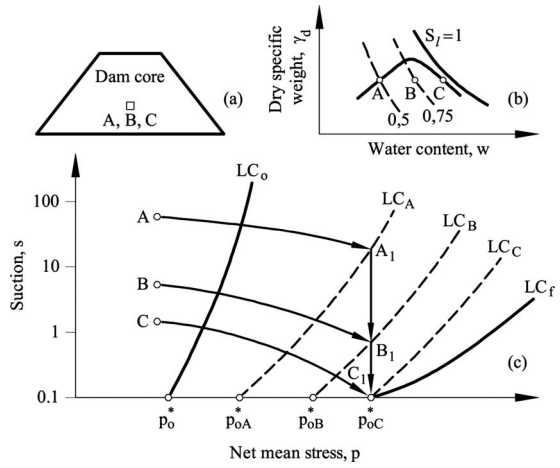

Fig. 11. (a) Alternative compaction conditions (A, B, C) at a given point within the core; (b) compaction plane; and (c) stress paths in (p, s) stress space

mation depend on soil type) allow the definition of the LC yield curves sketched.

Once this representation of the initial soil state is achieved it is possible to predict the soil behavior under the stress paths imposed by the dam construction and operation. The effect of changing compaction conditions is just a matter of changing the initial conditions.

The knowledge of initial conditions requires a limited amount of testing. All that is required is to know the water retention curve and an estimation of the preconsolidation stress (as shown in oedometer or isotropic loading; see also Alonso and Pinyol (2008) for correlations with γ_d and soil type). The important point to be stressed, however, is that, once this representation is achieved, all aspects of compacted soil behavior are consistently taken into account. Therefore, a sensitivity analysis on the effect of compaction conditions on dam core behavior, for instance, becomes a straightforward exercise.

Consider, in this regard, the example given in Fig. 11. The objective is now to predict the core behaviour for three alternative compaction conditions (A, B, and C, defined in Fig. 11(b), they are characterized by a common dry density and different water contents). The representation of the initial states is given in Fig. 11(c) (points A, B, C, and the associated yield state LC_0, which is defined by the common dry density).

Consider now the stress path induced by dam construction: The net mean stress will increase at a certain rate. p will increase and the reduction in void ratio will also imply some increase in degree of saturation which implies a suction reduction. The final stress states at the end of construction (A_1, B_1, C_1) will be located on the three yield curves indicated (LC_A, LC_B, LC_C) which have been dragged towards the right by the stress paths. An eventual wetting (suction reduction, due to water impoundment) will bring the current LC yield curves to a saturated state, which belongs to the final yield locus LC_f. The calculated collapse will be maximum for state A and minimum (or even some swelling; it will depend on model parameters) for initial state C.

These ideas have been illustrated in the context of the Lechago dam. Two new simulations, besides the one presented above, were performed considering dry and wet of the optimum compaction conditions. The assumption is now made that the dry density is maintained and the compaction water content changes (from dry to wet conditions). Table 6 specifies the assumed initial suctions for the dry and wet conditions, as well as the degree of saturation derived from the water retention relationship.

Figure 12 presents the distribution of degree of saturation in the core at the end of construction for the three conditions. The wet core becomes almost saturated at the end of construction. However, positive pore pressures develop only in the lower part of the core. (Fig. 13). Small negative pressures (within the range of the air entry value in most of the core) are calculated. The core loses water towards the rockfill shoulders in the cases solved. At

Table 6. Initial Conditions for Parametric Study on Compaction Conditions

Compaction condition	S_{l0} (%)	s_0 (MPa)
Dry core	55	15.0
Core at $w_{\text{opt.+2.7\%}}$	75	3.0
Wet core	90	0.8

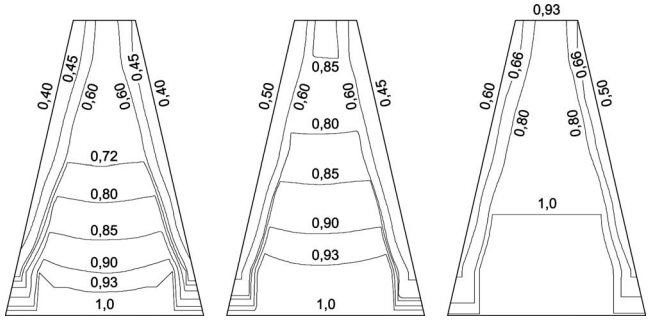

Fig. 12. Distribution of degree of saturation in the core at the end of construction: (a) dry core; (b) core at $w_{\text{opt.+2,7\%}}$; and (c) wet core

J. Geotech. Geoenviron. Eng., 2009, 135(7): 851-862

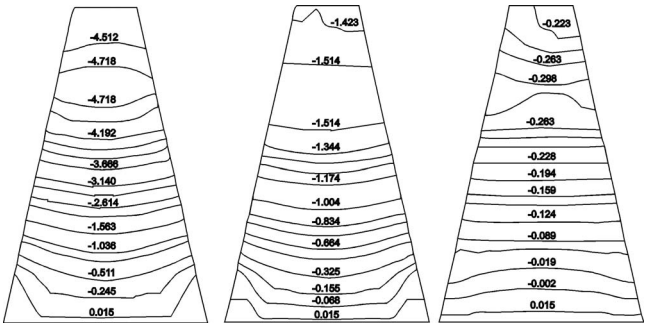

Fig. 13. Distribution of pore water pressure in the core at the end of construction: (a) dry core; (b) core at $w_{\text{opt.+2,7\%}}$; and (c) wet core

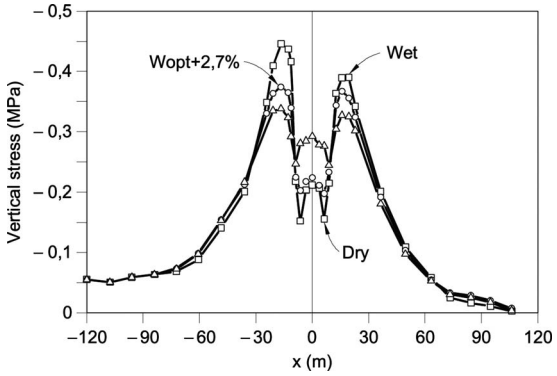

Fig. 15. Vertical stress in the horizontal section AB at the end of construction

the end of construction the dry core maintains degrees of saturation, in the range of 0.6 (upper part) to 0.9 (lower part) and high suctions.

Changes of degree of saturation and pore pressure are always controlled by the specific shape of the water retention curve. These two variables are always located on the water retention curve. It is also interesting to realize the coupled nature of phenomena since changes in degree of saturation affect directly the permeability, which in turn, controls the distribution of water pressures.

Figure 14 shows the distribution of vertical settlements along the dam axis at the end of construction for the three compaction conditions. Higher settlements are calculated for the wet core, which presents the maximum at a higher height than the two other cases. This is explained because the lower suctions associated with wet conditions imply a higher compressibility and a lower yielding stress [Eqs. (11) and (10) of the Appendix].

The influence of compaction water content in the development of the arching effect is presented in Fig. 15. The wet core is more deformable and the stress transfer mechanism is more pronounced. On the other hand, the dry core is more rigid and the arching effect is less developed.

The effective stress paths of a point located at the base of the clay core [element 758 in Fig. 1(b)] is shown in Fig. 16. Two cases have been plotted and they correspond to optimum and dry of optimum compaction conditions. At the end of construction, the bottom of the core is essentially saturated, when the clay is compacted at the optimum [Fig. 16(c)]. However, the dry of optimum material maintains a suction close to 0.7 MPa. When the dam is impounded (the transition is marked in the figure) there is an initial rapid reduction in suction due to the hydrostatic load on the upstream face of the core. The subsequent filtration and consolidation process saturates progressively the core material.

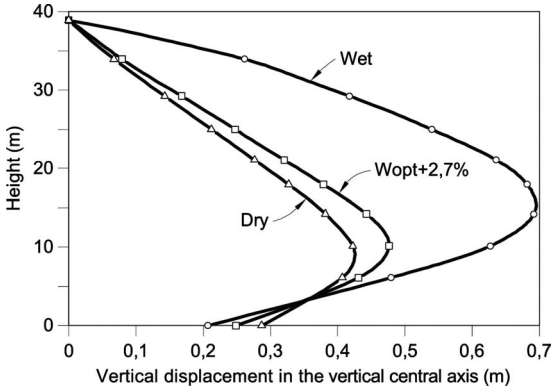

Fig. 14. Vertical displacement distribution in the central axis at the end of construction

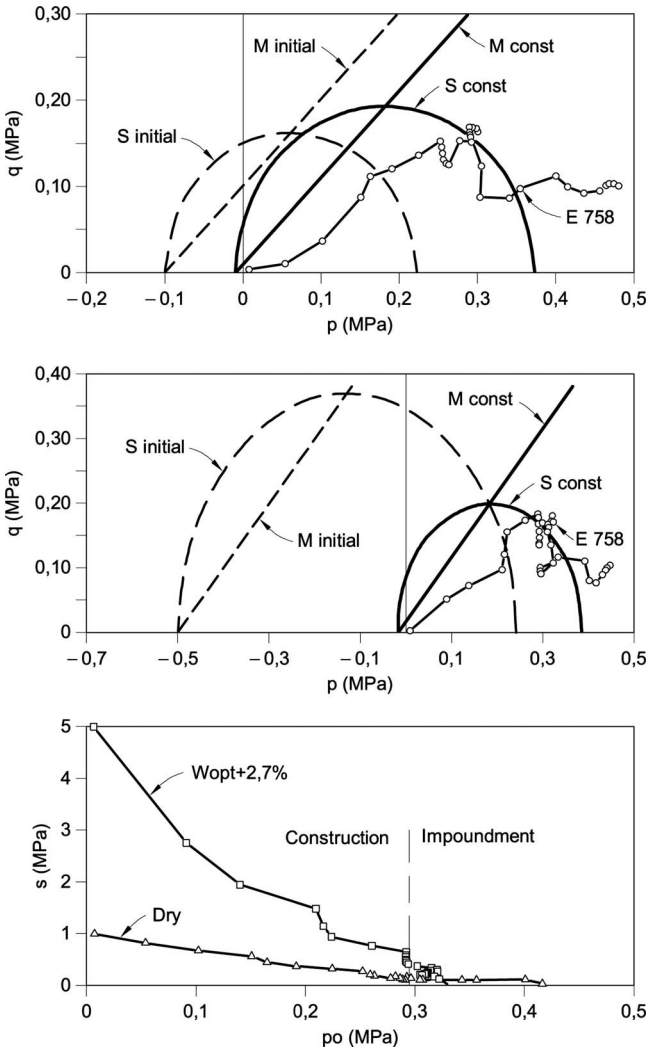

Fig. 16. Stress paths of element 758 (core) in (p,q) and (p,s) planes: (a) compaction water content=optimum+2.7%; (b) compaction water content=dry; and (c) stress paths in (p,s) stress space

J. Geotech. Geoenviron. Eng., 2009, 135(7): 851-862

Stress paths in the deviatoric plane are given in Figs. 16(a and b) for optimum and dry of the optimum compaction conditions. Also indicated in the plots are initial yield surface and the yield surface at the end of construction. The strong reduction in suction results in a significant shrinkage of the yield locus. During construction, the reference point follows approximately a K_0 path. Irregularities in the path are a consequence of the preloading sequence described before. Impoundment leads, for both compaction conditions, to a significant reduction of deviatoric stress. Mean net stress increases and the representative stress point separates progressively from the strength envelope. In both cases the soil is yielding in compression and shear. In fact, yielding conditions were reached relatively early in this point at some intermediate time during the construction process, as shown in both plots [Figs. 16(a and b)].

Conclusions

The paper describes a coupled flow-deformation analysis of the construction and impounding of the Lechago dam, which is presently under construction. Numerical simulations have been carried out with the computational code CODE_BRIGHT (Olivella et al. 1996), developed at the Department of Civil Engineering of UPC. Core and rockfill parameters were established by back-analysis of laboratory tests, in which loading and wetting paths were imposed. A good agreement between laboratory results and model calculations was achieved.

Simulation of dam construction shows the influence of suction in soil strength and stiffness. The results also show that permeability at the end of construction controls water infiltration through the core during impoundment. Changes in degree of saturation and water pressure pointed out how relevant are the water retention curve and nonlinear variation of permeability.

It has been shown that model parameters may be derived from a relatively simple set of laboratory tests. The expected dam behavior described on this paper constitutes a prediction exercise. It is expected that a comparison with the dam behavior, presently under construction, will provide an improved insight into the capabilities and limitations of the described approach.

The paper stresses also the advantages of modeling compacted soil behavior using concepts of unsaturated soil behavior in conjunction with an elastoplastic modeling of compacted soil behavior. It was shown that the initial compaction conditions, which, in practice, are characterized by a dry specific weight and water content, could be alternatively described by a yield stress and a matric suction. This is a fundamental description which opens the possibility of examining the effect of varying compaction conditions at a limited experimental and computational effort. The parametric study of the performance of the dam for three compaction states of the clay core demonstrated the capabilities of the procedure developed. Changes in a variety of properties (permeability, water retention properties, stiffness, yielding conditions, strength) are then automatically incorporated into the analysis.

The analysis presented indicated that the core compacted at the dry of the optimum water content is more rigid, stress transfer is less pronounced and foundation differential settlements are smaller. On the other hand, considerable suction values remain at the end of construction. They lead to low permeability values, which requires a longer time to reach steady-state condition after impounding. It is also emphasized that dry core presents a higher collapse potential during impounding. A similar, but in many aspects opposite, description could be made of the dam behavior for compaction wet of optimum.

Certainly, these are expected behaviors. But the modeling approach described provides a tool to investigate these effects in detail and in a consistent manner.

Acknowledgments

One of the writers (L. M. C.) is grateful to CNPq/Brazil for the financial support received for the development of the research reported in this paper.

Appendix. BBM Model

The model describes the mechanical behavior of partially saturated soils, especially those being moderately expansive or nonexpansive. It was described in Alonso, Gens, and Josa (1990). It is formulated in terms of two stress fields: the net stress (excess of total stress over air pressure, $\sigma_{ij}-p_a\delta_{ij}$) and the matric suction, $s=(p_a-p_w)\delta_{ij}$

The model is formulated within the framework of hardening plasticity and it becomes modified Cam-clay when suction is zero. The following set of equations describes the core of the model and the meaning of material parameters. Equations are given for a triaxial stress state defined by the following stress variables:

$$p = \sigma_m - \max(p_a, p_w); \quad \sigma_m = (\sigma_1 + \sigma_2 + \sigma_3)/3 \tag{9a}$$

$$s = p_a - p_w \tag{9b}$$

$$q = \sigma_1 - \sigma_3 \tag{9c}$$

where $\sigma_1, \sigma_2, \sigma_3$=total principal stresses. The net mean stress p is defined in the manner indicated in Eq. (9*a*) to facilitate the transition from unsaturated to saturated states. When the soil becomes saturated the model is formulated in terms of Terzaghi effective stress.

The model simulates the increase in strength with suction. For isotropic conditions, yield states associated with suction are described by means of a yield function defined in the space (p,s), which is named LC (after loading-collapse). It explains the collapse upon wetting and the increase of apparent preconsolidation stress $p_0(s)$ with suction through the following relationship:

$$p_0(s) = p^c\left(\frac{p_0^*}{p^c}\right)^{[\lambda(0)-\kappa]/[\lambda(s)-\kappa]} \tag{10}$$

where p_0^*=isotropic preconsolidation stress for saturated conditions; p^c=reference stress; κ=isotropic elastic compressibility defined below; and

$$\lambda(s) = \lambda(0)[(1-r)\exp(-\beta s) + r] \tag{11}$$

is the soil compressibility (elastoplastic) defined as

$$d\varepsilon_v = \frac{\lambda(s)}{1+e}\frac{dp}{p} \tag{12}$$

In Eq. (11), $\lambda(0)$=compressibility coefficient for saturated conditions β determinates the rate increase of stiffness with suction and r determinates the maximum soil stiffness.

An isotropic volumetric hardening law:

J. Geotech. Geoenviron. Eng., 2009, 135(7): 851-862

$$\frac{dp_0^*}{p_0^*} = \frac{1+e}{\lambda(0)-\kappa} d\varepsilon_v^p \tag{13}$$

defines the increase of the elastic domain.

A tensile strength increasing linearly with suction is defined:

$$p_s(s) = ks \tag{14}$$

where k=constant.

The yield surface LC is extended to triaxial conditions through the following family of ellipses:

$$q^2 - M^2[p + p_s(s)][p_o(s) - p] = 0 \tag{15}$$

where M=slope of the limiting critical state line. A nonassociated plastic potential provides the flow rule:

$$\frac{d\varepsilon_s^p}{d\varepsilon_v^p} = \frac{2q\alpha}{M^2[2p + p_s(s) + p_o(s)]} \tag{16}$$

where α=parameter (if $\alpha=1$, the flow rule is associated)

Elastic strains are induced by changes in net mean stress, deviatoric stress and suction according to the expression

$$d\varepsilon^e = \frac{\kappa}{(1+e)}\frac{dp}{p} + \frac{1}{3G}dq + \frac{\kappa_s}{(1+e)}\frac{ds}{(s+p_{\text{atm}})} \tag{17}$$

where G=shear modulus and κ, κ_s are compressibility coefficients against changes in net mean stress and suction.

References

Alonso, E. E. (1998). "Suction and moisture regimes in roadway bases and subgrades." *Proc., Int. Symp. On Internal Drainage of Pavements and Subgrades*, 57–104.

Alonso, E. E., and Batlle, F. (1995). "Construction and impoundment of an earthdam. Application of the coupled flow-deformation analysis of unsaturated soils." *CISM courses and lectures*, No. 357, Springer, Vienna.

Alonso, E. E., Batlle, F., Gens, A., and Lloret, A. (1988). "Consolidation analysis of partially saturated soils—Application to earthdam construction." *Int. Conf. on Numerical Methods in Geomechanics*, 1303–1308.

Alonso, E. E., Gens, A., and Hight, D. W. (1987). "Special problem soils." *Proc., 9th European Conf. Soil Mechanics and Foundation Engineering*, Vol. 3, 1087–1146.

Alonso, E. E., Gens, A., and Josa, A. (1990). "A constitutive model for partially saturated soils." *Geotechnique*, 40(3), 405–430.

Alonso, E. E., Lloret, A., Gens, A., Batlle, F., and Delahaye, C. H. (1995). "Effect of core compaction water content on the behaviour of earthdams." *Proc., 1st Int. Conf. on Unsaturated Soils*, Vol. 1, 231–239.

Alonso, E. E., Olivella, S., and Pinyol, N. M. (2006). "A review of Beliche Dam." *Geotechnique*, 55(4), 267–285.

Alonso, E. E., and Pinyol, N. M. (2008). "Unsaturated soil mechanics in earth and rockfill dam engineering." Opening Lecture. *Proc., 1st European Conf. on Unsaturated Soils*, Durham, U.K., 3–32.

Aubry, D., Ozanam, O., and Person, J. P. (1987). "Ecoulements non saturés en milieux poreux deformables." *Proc., 9th European Conf. on Soil Mechanics and Foundation Engineering*, Vol. 2, 537–540.

Bonelli, S., and Poulain, D. (1995). "Unsaturated elastoplastic model applied to homogeneous earthdam behaviour." *Proc., 1st Int. Conf. on Unsaturated Soils*, Vol. 1, 265–272.

Cavounidis, S. (1975). "Effective stress-strain analysis of earth dams during construction." *Thesis Presented to Stanford University, Technical Rep. No. 201*.

Chang, C. S., and Duncan, J. M. (1977). "Analysis of consolidation of earth and rockfill dams." *Rep. No TE 77-3*, Dept. of Civil Engineering, Univ. of California, Berkeley.

Chávez, C., and Alonso, E. E. (2003). "A constitutive model for crushed granular aggregates which includes suction effects." *Soils Found.*, 43(4), 215–228.

Costa, L. M. da (2000). "Análise hidro-mecânica de solos não saturados com aplicação a barragem de terra." Doctoral thesis, COPPE/UFRJ, Rio de Janeiro.

DIT-UPC, CODE_BRIGHT. (2002). "A 3D program for thermo-hydro-mechanical analysis in geological media." *User's guide*, CIMNE, Barcelona.

Eisenstein, Z., and Law, S. T. C. (1977). "Analysis of consolidation behaviour of Mica dam." *J. Geotech. Engrg. Div.*, 103, 879–895.

Fry, J. J., Charles, J. A., and Penman, A. D. M. (1996). "Dams, embankments and slopes." *Proc., the 1st Int. Conf. on Unsaturated Soils*, Vol. 3, 1391–1419.

Gatmiri, B., Tavakoli, S., Moussavi, J., and Delage, P. (1995). "Numerical approach of elastoplastic consolidation of unsaturated soils." *Proc. 1st Int. Conf. on Unsaturated Soils*, Vol. 2, 1057–1064.

Gens, A., Garcia-Molina, A. J., and Guimarães, L. N. (1997). "Preoperational thermo-hydro-mechanical (THM) modelling of the 'Mockup' test." *Rep. by ENRESA-FEBEX 70-UPC-M-3-002*.

Ghaboussi, J., and Kim, K. J. (1982). "Analysis of saturated and partially saturated soils." *Int. Symp. on Numerical Models in Geomechanics*, 377–390.

Holtz, R. D., and Kovacs, W. D. (1981). "An introduction to geotechnical engineering." Prentice-Hall, Englewood Cliffs, N.J.

Justo, J. L., and Saura, J. (1983). "Three-dimensional analysis of Infiernillo dam during construction and filling of the reservoir." *Int. J. Numer. Analyt. Meth. Geomech.*, 7(2), 225–243.

Kogho, Y. (1992). "Deformation analysis of fill type dams during reservoir filling." *Proc., 4th Int. Symp. Numerical Models in Geomechanics*, Vol. 2, 777–787.

Kogho, Y. (2003). "Review of constitutive models for unsaturated soils." *Proc. 2nd Asian Conf. on Unsaturated Soils*, Osaka, 21–40.

Kogho, Y., and Yamashita, T. (1988). "Finite element analysis of fill type dams—Stability during construction by using the effective stress concept." *Int. Conf. on Numerical Methods in Geomechanics*, 1315–1322.

Laigle, F., Poulain, D., and Magnin, P. (1995). "Numerical simulation of La Ganne dam behaviour by a three phases approach." *Proc., 1st Int. Conf. on Unsaturated Soils*, Vol. 2, 1101–1108.

Ledesma, A., Chan, A. H. C., Vaunat, J., and Gens, A. (1995). "Finite element formulation of an elastoplastic model for partially saturated soils," *Proc., 4th Int. Conf. on Computational Plasticity*, 1677–1688.

Lloret, A., and Alonso, E. E. (1985). "State surfaces for partially saturated soils." *Proc., 11th Int. Conf. on Soil Mechanics and Foundation Engineering*, Vol. 2, 557–562.

Matyas, E. L., and Radhakrishna, H. S. (1969). "Volume change characteristics of partially saturated soils." *Geotechnique*, 18(4), 432–448.

Naylor, D. J., Maranha das Neves, E., Mattar, D., Jr., and Veiga Pinto, A. A. (1986). "Prediction of construction performance of Beliche Dam." *Geotechnique*, 36(3), 359–376.

Naylor, D. J., Maranha das Neves, E., and Veiga Pinto, A. A. (1997). "A back-analysis of Beliche Dam." *Geotechnique*, 47(2), 221–233.

Naylor, D. J., Tong, S. L., and Shahkarami, A. A. (1989). "Numerical modelling of saturation shrinkage." *Proc. 3rd Int. Symp. On Numerical Models in Geomechanics*, Niagara Falls, 636–648.

Ng, K. L. A., and Small, J. C. (1995). "Simulation of dams constructed with unsaturated fills during construction and water impounding." *Proc., 1st Int. Conf. on Unsaturated Soils*, Vol. 1, 281–286.

Nobari, E., and Duncan, J. (1972). "Effect of reservoir filling on stresses and movements in earth and rockfill dams." *Rep. No. TE-72-1*, Berkeley: Office of Research Services, University of California, 1–186.

Oldecop, L. A., and Alonso, E. E. (2001). "A model for rockfill compressibility." *Geotechnique*, 51(2), 127–139.

J. Geotech. Geoenviron. Eng., 2009, 135(7): 851-862

Olivella, S., Carrera, J., Gens, A., and Alonso, E. E. (1994). "Nonisothermal multiphase flow of brine and gas through saline media." *Transp. Porous Media*, 15, 271–293.

Olivella, S., Gens, A., Carrera, J., and Alonso, E. E. (1996). "Numerical Analysis for a simulator (CODE_BRIGHT) for the coupled analysis of saline media." *Eng. Comput.*, 13, 87–112.

Richards, B. G., and Chang, C. Y. (1969). "Prediction of pore pressures in earth dams." *Proc., 7th Int. Conf. on Soil Mechanics and Foundation Engineering*, 2, 355–362.

Sivakumar, V., and Wheeler, S. J. (2000). "Influence of compaction procedure on the mechanical behaviour of an unsaturated compacted clay. Part 1: Wetting and isotropic compression." *Geotechnique*, 50(4), 359–368.

Skempton, A. W. (1954). "The pore pressure coefficients A and B," *Geotechnique*, 4(4), 143–147.

Smith, I. M., and Hobbs, R. (1976). "Biot analysis of consolidation beneath embankments." *Geotechnique*, 26(1), 149–171.

Soriano, A., Sánchez, F. J. and Serrano, C. (1990). "Simulation of wetting deformations of rockfills." *Proc., 2nd Eur. Conf. on Numer. Methods in Geotech. Engng.*, Santander, 495–517.

Van Genutchen, M. T. (1980). "A closed form equation for predicting the hydraulic conductivity of unsaturated soils." *Soil Sci. Soc. Am. J.*, 44, 892–898.

Veiga Pinto, A. A. (1983). "Previsão do comportamento estrutural de barragens de aterro." Thesis, LNEC, Lisbon.